GEOCHEMISTRY AND GEOTECTONIC SIGNIFICANCE OF NEOPROTEROZOIC OPHIOLITIC PERIDOTITES AND PYROXENITES: KAB AMIRI, EASTERN DESERT, EGYPT

Sherif Kharbish[1, *] Amr El-Awady[2]

[1] Prof. Dr. rer. nat. Sherif Kharbish, Geology Department, Faculty of Science, Suez University, Suez Governorate, El Salam City, 43518, Egypt. *corresponding author e-mail: sherif.kharbish@suezuni.edu.eg

[2] Dr. Amr El-Awady, PhD., Geology department, Faculty of Science, Zagazig University, Zagazig, Egypt.

DOI http://doi.org/10.24040/actaem.2017.20.1.38-45

Abstract: The Kab Amiri ultramafic ophiolitic section comprises highly serpentinites and pyroxenites. The Kab Amiri ophiolite suite represents fragments of oceanic lithosphere that are developed in forearc setting in a supra-subduction zone environment. The clinopyroxenes chemistry reflect the strong affinity of pyroxenitestoward the intra-oceanic forearc boninites. Serpentinites have been most likely formed directly from mantle-wedge olivine above the slab in which the fluids driven for the slab cause strong hydration and cooling of peridotites during an early stage of serpentinization. Pyroxenites show a very close relation to the serpentinites, which reflect that both are co-genetic with the rest of the mantle suite. Thus, the pyroxenites genesis is directly related to the contamination of their mantle source by crustal material and/or subduction-related slab fluids during mantle evolution in supra subduction zone setting.

Key words: Neoproterozoic; ophiolites; forearc; Raman spectroscopy; Egypt

Introduction

The Egyptian Neoproterozoic ophiolites (ENO) (e.g. Farahat et al., 2004; Stern et al., 2004) were considered to be generated in mid-ocean ridges (e.g. Zimmer et al., 1995), or formed in a forearc (e.g. Stern et al. 2004) or a back-arc setting (e.g. Farahat et al., 2004). The Kab Amiri district (KAD), central Eastern Desert (CED), Egypt, was long known as a small Au mining district since ancient times (Andráš and Kharbish, 2014), which dates back to New ancient Egyptian (Pharaonic) dynastic Kingdoms (2700 to 1070 BC) (Kharbish and Andráš, 2014a, b). Despite the work that has been done on the different rock units in the KAD, few detailed investigations on the ENO in the KAD area, were performed. Thence, the present article goals to establish the primary petrography and bulk-rock geochemistry of ENO in the KAD area. This study uncovered a good model for the sophisticated geologic processes experienced by the Egyptian Neoproterozoic ophiolitic rocks, notwithstanding the tricky task of eliciting information from these complex rocks.

Geology and petrography

The KAD area is ~ 45 km far from Port Quseir in the CED of Egypt and lies within a region (from oldest to youngest, Fig. 1a) of Neoproterozoic ophiolitic rocks and associated derivatives that are emplaced in island arc, calc-alkaline volcano-sedimentary associations (Fig. 1b) and metagabbro-diorite assemblages (older gabbros), which together with the ophiolitic suites were later intruded by older granitoids and younger granites (Moghazi, 2002).

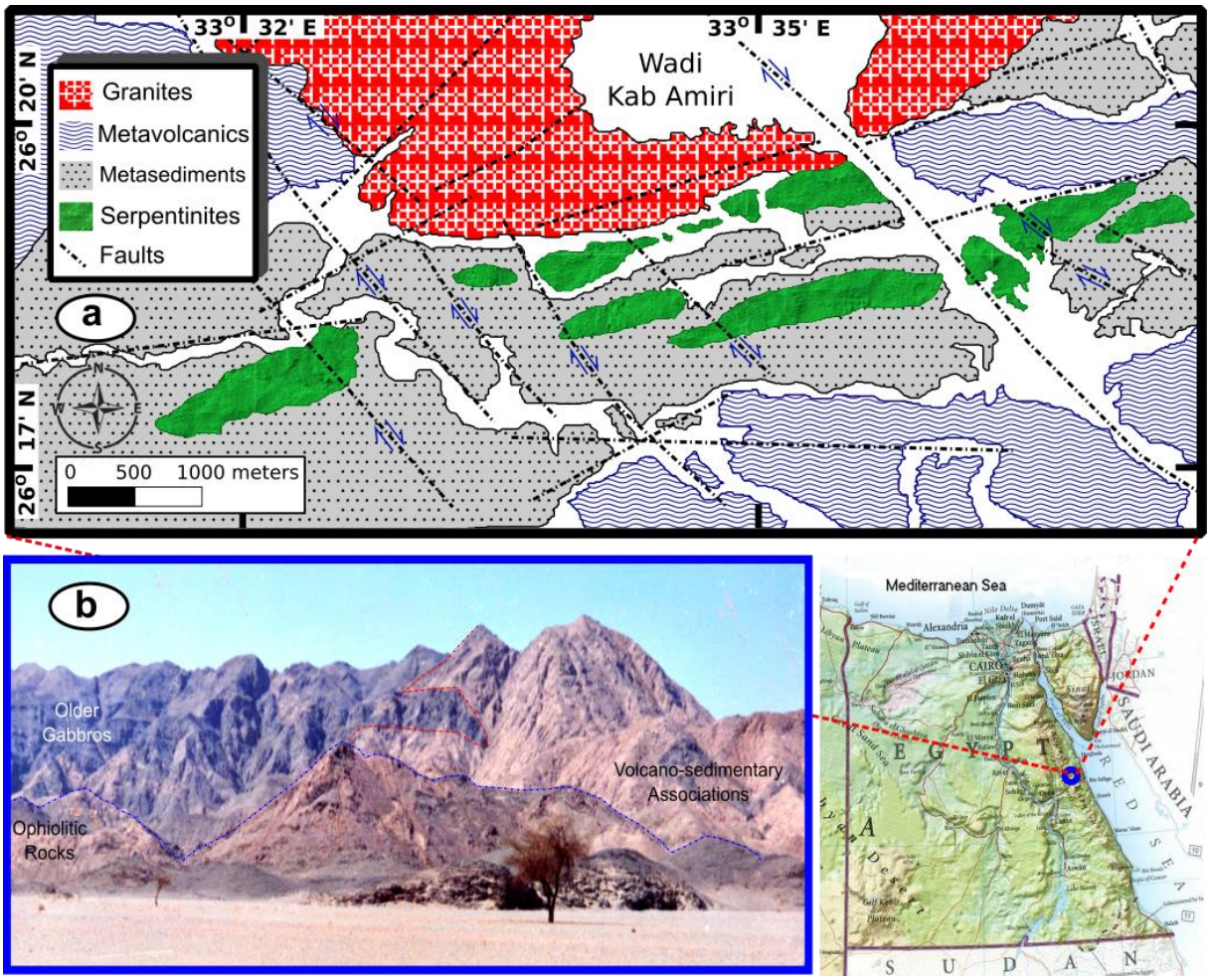

Fig 1 Geological map of G. Kharaza area Fig. 1. (a) Geological map of Kab Amiri area, Eastern Desert, Egypt and (b) Contact between the serpentinites and the underlying volcano-sedimentary rocks.

The KAD serpentinites (highly serpentinized peridotites) display a massive fine- to medium-grained appearance and grayish to greenish colors. Petrographically, serpentinites compose basically of fine- to medium-grained platy shreds and fibrous flakes antigorite, together with primary chromian spinel and few amounts of secondary metamorphic minerals talc and chlorite. The rocks commonly preserve pseudomorphic textures of serpentine after orthopyroxene (bastite texture) that testify their harzburgite parentage. Subhedral shape spinel crystals (altered along fractures and grain boundaries) exhibit three irregular optical zoning owing to their alteration processes. Rarely chlorite grains occur as small aggregates in a serpentine matrix or as aureoles around altered chromian spinel. Pockets or small elongated massive remnants are recorded within the serpentinites that consist mainly of pyroxenites. The pyroxenites are predominantly composed of clinopyroxene (diopside + rare augit) and orthopyroxene (enstatite), with antigorite and subordinate amounts of metamorphic minerals (viz., tremolite, talc and chlorite).

Samples and experiments

Minerals compositions were obtained by the Cameca microbeam electron microprobe analyzer (EMPA; Cameca SX 100), with 15 Kv accelerating voltage, 20 nA beam current, 1 μm beam diameter and a counting time of 10s. Representative 20 samples (10 serpentinites and 10 pyroxenites) from the KAD area have been analyzed for their major, and trace compositions. Analyses were performed by the X-ray spectrometer Phillips PW 2400. Analytical precision was better than 1% and 3% for major and trace elements, respectively.

Results

The MgO contents and LOI are much higher in serpentinites compared with those in pyroxenites; whereas the higher values of CaO content occur in pyroxenites (Tab 1). The serpentinites plot in within the harzburgite field (Fig 2a), whereas the pyroxenites lie within the olivine websterite field (Fig 2a). KAD serpentinites and pyroxenites are closely associated or connected with the ophiolitic peridotite (Fig. 2b).

Both serpentinites and pyroxenites show depleted to highly depleted trace elements patterns relative to the primitive mantle (Fig 2c). The great likeness among the trace element patterns of the examined rocks indicate the genetic connection of serpentinites and pyroxenites.

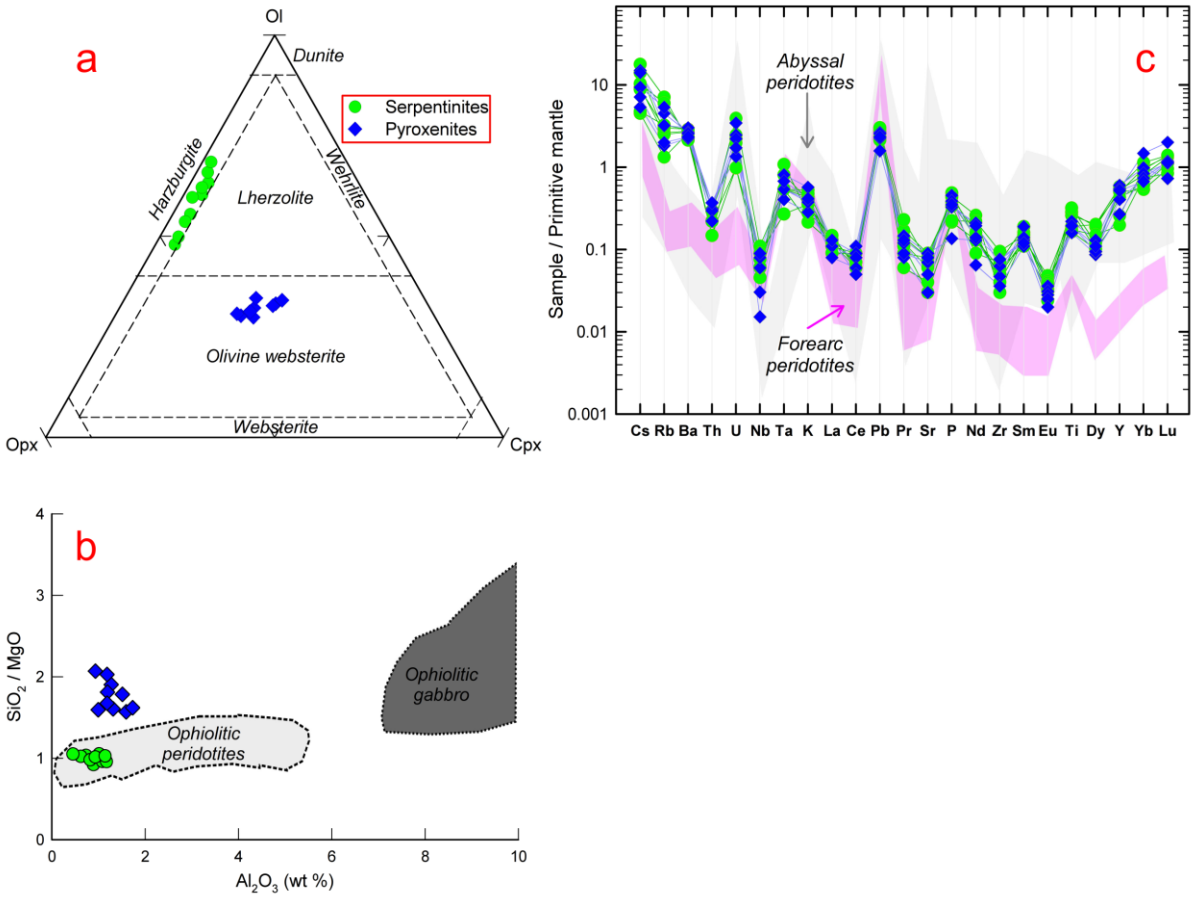

Fig 2 (a) Ol–Cpx–Opx classification diagram (Streckeisen, 1976), (b) relationship between Al_2O_3 wt.% and SiO_2 /MgO of the studied rocks (MORB, ophiolitic gabbros and ophiolitic peridotites fields after Bodinier and Godard, 2003) and (c) primitive mantle-normalized trace element patterns (Normalizing values after McDonough and Sun 1995; Compositional ranges for ancient and modern forearc peridotites after Song et al. 2009).

Tab 1 Whole rock major (wt.%), trace and rare-earth element (ppm) data of Kab Amiri district rocks.

	Se1	Se2	Se3	Se4	Se5	Se6	Se7	Se8	Se9	Se10
	Serpentinite (wt %)									
SiO_2	41.62	40.25	38.85	37.62	39.52	40.61	38.65	39.52	40.36	40.05
TiO_2	0.04	0.11	0.07	0.05	0.06	0.03	0.02	0.04	0.08	0.10
Al_2O_3	0.73	0.62	0.89	1.08	0.45	1.01	0.82	1.17	0.93	1.14
Fe_2O_3	8.36	8.11	7.06	9.02	8.75	9.64	8.72	7.95	9.73	8.95
MgO	40.23	39.36	42.15	39.12	37.58	38.56	39.36	41.23	39.75	38.95
MnO	0.12	0.34	0.26	0.11	0.15	0.14	0.13	0.37	0.24	.011
CaO	0.65	0.69	0.62	0.82	0.67	0.73	0.59	0.72	0.76	0.59
Na^2O	0.05	0.07	0.03	0.05	0.03	0.20	0.07	0.05	0.09	0.11
K_2O	0.02	0.01	0.05	0.09	0.04	0.03	0.03	0.09	0.05	0.02
P_2O_5	0.04	0.08	0.06	0.02	0.07	0.02	0.04	0.04	0.09	0.03
LOI	7.23	10.28	9.77	11.89	12.19	8.76	11.06	8.49	7.63	9.38
Total	**99.09**	**99.92**	**99.81**	**99.87**	**99.51**	**99.73**	**99.49**	**99.67**	**99.71**	**99.43**

	Se1	Se2	Se3	Se4	Se5	Se6	Se7	Se8	Se9	Se10
						ppm				
Ba	10	8	9	8	7	10	8	9	7	8
Cs	0.4	0.3	0.4	0.2	0.4	0.3	0.1	0.3	0.5	0.1
Nb	1	2	2	1	2	1	1	1	2	2
Pb	3	3	3	4	4	3	3	4	3	3
Rb	2	2	3	2	1	2	2	1	2	2
Sr	58	57	51	38	49	28	33	51	57	54
Ta	2	3	3	3	2	2	3	2	3	2
Th	3	4	3	3	4	3	3	4	3	4
U	4	6	3	8	4	6	5	4	6	4
Y	0.185	0.211	0.325	0.258	0.421	0.369	0.732	0.584	0.474	0.240
Zr	4.8	6.1	3.0	4.1	4.6	5.0	3.7	6.0	4.0	3.5
La	0.14	0.23	0.26	0.28	0.34	0.18	0.26	0.37	0.18	0.24
Ce	5	5	5	6	6	5	6	6	6	5
Pr	0.056	0.042	0.031	0.147	0.062	0.063	0.047	0.073	0.029	0.010
Nd	0.28	0.17	0.57	0.48	0.41	0.44	0.54	0.42	0.55	
Sm	0.140	0.200	0.124	0.220	0.147	0.078	0.114	0.175	0.084	0.210
Eu	0.062	0.075	0.082	0.081	0.042	0.026	0.037	0.055	0.047	0.026
Dy	0.214	0.206	0.154	0.421	0.178	0.084	0.132	0.208	0.145	0.139
Yb	0.210	0.170	0.150	0.090	0.032	0.041	0.058	0.13	0.018	0.190
Lu	0.027	0.066	0.048	0.034	0.012	0.019	0.029	0.042	0.051	0.036
	Pe1	**Pe2**	**Pe3**	**Pe4**	**Pe5**	**Pe6**	**Pe7**	**Pe8**	**Pe9**	**Pe10**
					Pyroxenite (wt %)					
SiO_2	44.52	45.63	45.25	49.18	46.61	48.91	44.89	47.41	45.93	49.04
TiO_2	0.14	0.01	0.19	0.11	0.05	0.04	0.17	0.06	0.12	0.08
Al_2O_3	0.99	1.59	1.73	0.93	1.51	1.27	1.31	1.19	1.18	1.18
Fe_2O_3	8.28	7.98	8.46	7.25	8.81	7.63	8.37	7.62	8.64	7.44
MgO	27.89	29.05	27.94	23.76	26.11	25.69	27.92	26.17	27.40	24.16
MnO	0.21	0.16	0.14	0.16	0.22	0.18	0.19	0.16	0.18	0.17
CaO	13.33	12.14	10.75	14.22	13.51	12.25	12.04	13.18	12.13	13.23
Na^2O	0.05	0.07	0.12	0.05	0.06	0.03	0.07	0.06	0.09	0.04
K_2O	0.02	0.01	0.04	0.02	0.07	0.03	0.03	0.02	0.06	0.03
P_2O_5	0.02	0.01	0.03	0.02	0.05	0.02	0.02	0.01	0.04	0.02
LOI	3.79	3.02	4.52	3.94	2.54	3.77	4.24	3.48	3.94	3.86
Total	**99.42**	**99.67**	**99.17**	**99.64**	**99.54**	**99.82**	**99.25**	**99.36**	**99.71**	**99.25**
	Pe1	**Pe2**	**Pe3**	**Pe4**	**Pe5**	**Pe6**	**Pe7**	**Pe8**	**Pe9**	**Pe10**
						ppm				
Ba	14	10	27	25	26	48	10	37	45	76
Cs	0.2	0.4	0.3	0.4	0.2	0.4	0.3	0.2	0.5	0.4
Nb	2	2	4	4	4	2	2	2	3	2
Pb	4	6	8	5	4	11	11	8	9	6
Rb	2	2	2	2	6	11	7	8	6	5
Sr	13	14	13	19	105	184	116	9	210	173
Ta	3	3	3	3	3	3	6	4	3	4
Th	3	3	5	6	3	3	5	3	4	4
U	3	3	3	3	5	5	5	5	3	5
Y	3	2	2	7	4	2	12	10	2	15
Zr	22	24	35	52	68	25	33	24	64	73
La	5	18	22	11	6	8	9	9	11	20
Ce	8	13	6	19	31	16	6	21	14	24

Pr	0.28	0.34	0.18	0.26	0.37	0.18	0.24	0.27	0.23	0.26
Nd	0.47	0.28	0.17	0.57	0.48	0.18	0.34	0.21	0.74	0.57
Sm	0.05	0.04	0.05	0.07	0.05	0.04	0.01	0.03	0.04	0.07
Eu	0.03	0.02	0.01	0.03	0.03	0.03	0.04	0.01	0.02	0.02
Dy	0.12	0.11	0.10	0.14	0.12	0.11	0.14	0.08	0.12	0.17
Yb	0.09	0.09	0.10	0.10	0.20	0.20	0.10	0.10	0.20	0.09
Lu	0.02	0.01	0.02	0.01	0.06	0.03	0.05	0.04	0.04	0.01

Discussion

The chemistry of clinopyroxenes in pyroxenites reflect their strong affinity toward the intra-oceanic forearc boninites (Fig 3a, b). The Al_2O_3 contents and the FeO/MgO ratio of the parental melt and the empirical degree of partial melting (F) of the investigated chromian spinels in serpentinites were computed using the equations of Maurel and Maurel (1982) and Hellebrand et al., (2001), respectively. The obtained values of the parental melt Al_2O_3 (10.31 – 12.89 wt%), FeO/MgO (0.95 – 1.84) and F (19 - 22) are consistent with the composition of primary boninites [Al_2O_3 = 10.60–14.40 wt%, FeO/MgO = 0.70 – 1.40, (Wilson, 1989)] and the peridotites recovered from forearcs (F = 20-25; Zanetti et al., 2006). Furthermore, the depletion in Nb contents (Fig 2c) are similar to those in the forearc peridotites (Song et al., 2009).

One of the fundamental problems related to the study of serpentinites is the determination of their metamorphic grade. The presence of antigorite as the only serpentine mineral in serpentinites and the absence of newly formed olivine indicates that they were formed in the stability field of antigorite (250–600 °C; Evans 2004) or that the temperature did not exceed the lower amphibolite facies metamorphism range (i.e. below 500°C).

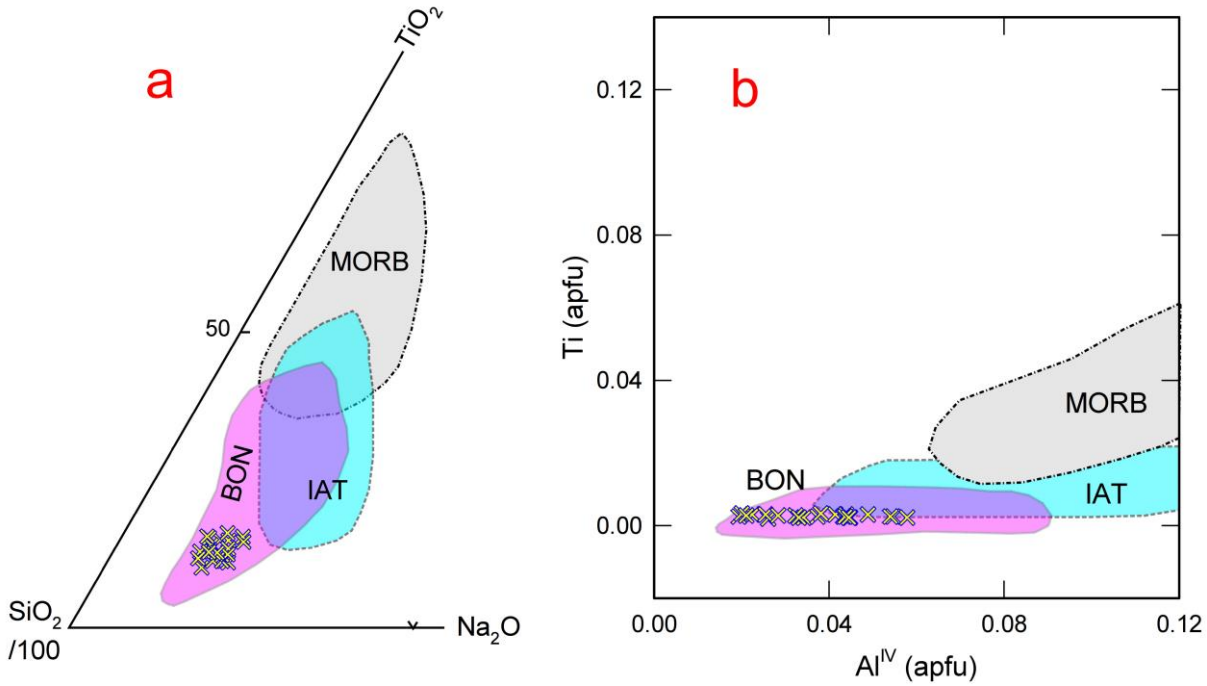

Fig. 3 Plot of the analyzed pyroxenes on (a) SiO_2 –TiO_2 –Na_2O diagram (Beccaluva et al., 1989) and (b) Ti vs. Al^{iv} diagram (Beccaluva et al., 1989).

Serpentinites have been most likely formed directly from mantle-wedge olivine above the slab in which the fluids driven for the slab cause strong hydration and cooling of peridotites during an early stage of serpentinization (400−600 °C; Khedr and Arai, 2010). Thus the antigorite formation usually occur at ~ 500°C (Moody, 1976), while the olivine after antigorite is commonly composed by dehydration at > 500ºC; (Caruso and Chernosky, 1979), which is the

minimum temperature for the ferrian chromite, antigorite and chlorite formation (Jan and Windley, 1990).

Many researchers have proposed that chromian spinel breakdown during metamorphism to form chlorite (Shen et al., 1988) at relatively high temperatures (> 400ºC; Kimball, 1990) and in the presence of aqueous fluids (Merlini et al., 2009); implies outward Al and Mg diffusion from chromian spinel, leaving a residual Fe^{3+}-enriched and Al-, Mg-depleted Cr-spinel (ferrian chromite) (Kimball, 1990; Merlini et al., 2009). The serpentinization of both pyroxene and olivine at temperatures between 200 and 300º C (Bach et al., 2006) could favor the creation of an aqueous fluid rich environment necessary for the chlorite and ferrian chromite formations.

At high oxidative conditions [i.e. increase in $f(O_2)$], the reaction of chromian spinel with serpentine favor to produce chlorite and Cr-magnetite (Mellini et al., 2005). This increase in the oxidative conditions (necessary for Cr-magnetite formation) may be took place after the late stages of serpentinization or during lower temperature amphibolite facies metamorphism (Bach et al., 2006).

The investigated pyroxenites display a very close relation to the serpentinites, which reflect that both are co-genetic with the rest of the mantle suite. Therefore, the KAD pyroxenites genesis could be related to the contamination of their mantle source by crustal material and/or subduction-related slab fluids during mantle evolution in supra subduction zone (SSZ) setting. Thus the low TiO_2 contents (0.07 -0.12 wt%, Table 1); the enrichment in LILE (Fig 2c) and LREE (Fig. 3d) and the Nb depletion (Fig 2c) indicate the remelting of a highly depleted mantle source and suggest their formation in a SSZ environment (i.e forearc).

References

Andráš, P., Kharbish, S. 2014. Gold sources in ancient Egypt. In: Andráš, P., Dirner, V., Kharbish, S. (Eds), *Historic deposits and their impact on environment*. 1St Ed., Technicka univerzita v Kosiciach Slovakia, ISBN 978-80-553-1756-4, 57-75.

Bach, W., Paulick, H., Garrido, C.J., Ildefonse, B., Meurer, W., Humphris, S.E. 2006. Unravelling the sequence of serpentinization reactions: petrography, mineral chemistry, and petrophysics of serpentinites from MAR 15oN (ODP Leg 209, Site 1274). *Geophysical Research Letters* 25, 1467-1470. DOI: https://doi.org/10.1029/2006GL025681

Beccaluva, L., Macciota, G., Piccardo, G.B., Zeda, O. 1989. Clinopyroxene composition of ophiolitic basalts as petrogenetic indicator. Chemical Geology 77, 165–182. DOI: https://doi.org/10.1016/0009-2541(89)90073-9

Bodinier, J.L., Godard, M. 2003. Orogenic, ophiolitic, and abyssal peridotites. In: Carlson, R.W. (Ed.), *Treatise on Geochemistry Mantle and core: Treatise on Geochemistry 2*. Elsevier Science Ltd, 103–170.

Caruso, L.J., Chernosky, J.V. Jr. 1979. The stability of lizardite. *Canadian Mineralogist*, 17, 757–770.

Evans, B.W. 2004. The Serpentinite Multisystem Revisited: Chrysotile Is Metastable. *International Geology Review*, 46, 479–506. DOI: https://doi.org/10.2747/0020-6814.46.6.479

Farahat, E.S., El-Mahalawi, M.M., Hoinkes, G. 2004. Continental back-arc basin origin of some ophiolites from the Eastern Desert of Egypt. *Mineralogy and Petrology*, 82, 81–104. DOI 10.1007/s00710-004-0052-6

Hellebrand, E., Snow, J.E., Dick, H.J.B., Hofmann, A.W. 2001. Coupled major and trace elements as indicators of the extent of melting in mid-ocean-ridge peridotites. *Nature*, 410, 677-681. DOI: 10.1038/35070546

Jan, M.Q., Windley, B.F. 1990. Chromian spinel-silicate chemistry in ultramfic rocks of the Jijal Complex, northwest Pakistan. *Journal of Petrology*, 31, 67–71. DOI: https://doi.org/10.1093/petrology/31.3.667

Kharbish, S., Andráš, P., 2014a. Exploitation of ores, rocks and minerals in ancient Egypt. *Acta Universitatis Matthiae Belii, seria Environmentalne Manažérstvo*, 1, 24 – 33.

Kharbish, S., Andráš, P., 2014b. Pharaonic Egypt mines and quarries. In: Andráš, P., Dirner, V., Kharbish, S. (Eds), *Historic deposits and their impact on environment.* 1St Ed., Technicka univerzita v Kosiciach Slovakia, ISBN 978-80-553-1756-4, 36 – 57.

Khedr, M.Z., Arai, S. 2010. Hydrous peridotites with Ti-rich chromian spinel as a low-temperature forearc mantle facies: evidence from the Happo-O'ne metaperidotites (Japan). *Contribution to Mineralogy and Petrology*, 159, 137–157.

Kimball, K.L. 1990. Effects of hydrothermal alteration on the composition of chromian spinels. *Contributions to Mineralogy and Petrology*, 105, 337-346.

Maurel, C., Maurel, O., 1982. Étude experimentale de la distribution de l'aluminiun entre bain silicaté basique et spinelle chromifére. Implications pétrogénétiques: teneur en chrome des spineless. *Bulletin de Minéralogie*, 105, 197-202.

McDonough, W.F., Sun, S.S., 1995. The composition of the earth. *Chemical Geology*, 120, 223–253. DOI: https://doi.org/10.1016/0009-2541(94)00140-4

Mellini, M., Rumori, C., Viti, C. 2005. Hydrothermally reset magmatic spines in retrograde serpentinites: formation of "ferritchromit" rims and chlorite aureoles. *Contributions to Mineralogy and Petrology*, 149, 266-275.

Merlini, A., Grieco, G., Diella, V. 2009. Ferritchromite and chromian-chlorite formation in mélange-hosted Kalkan chromitite (Southern Urals, Russia). *American Mineralogist*, 94, 1459–1467. DOI: 10.2138/am.2009.3082

Moghazi, A.M. 2002. Petrology and geochemistry of Pan-African granitoids, Kab Amiri area, Egypt – implications for tectonomagmatic stages in the Nubian Shield evolution. *Mineralogy and Petrology*, 75, 41–67.

Shen, P., Hwang, S.L., Chu, H.T., Jeng, R.C. 1988. STEM study of ''ferritchromit'' from the Heng-Chun chromitite. *American Mineralogist*, 73, 383–388.

Song S.G., Niu, Y.L m., Zhang, L.F.m – Bucher, K., 2009. The Luliangshan garnet peridotite massif of the North Qaidam UHPM belt, NW China – a review of its origin and metamorphic evolution. *Journal of Metamorphic Geology*, 27, 621–638. DOI: https://doi.org/10.1111/j.1525-1314.2009.00848.x

Stern, R.J., Johnson, P.R., Kröner, A., Yibas, B. 2004. Neoproterozoic ophiolites of the Arabian–Nubian Shield. In: Kusky, T.M. (Ed.). *Precambrian Ophiolites and Related Rocks. Development of Precambrian Geology*, 13, 95–128.

Streckeisen, A. 1976. Classification of common igneous rocks by mean of their chemical composition. A provisional attempt. *Neues Jahrbuch für Mineralogie – Abhandlungen*, 1–15.

Wilson, M. 1989. *Igneous petrogenesis.* London: U.K., Unwin Hyman, 466 pp.

Zanetti, A., d'Antonio, M., Spadea, P., Raffone, N., Vannucci, R., Bruguier, O., 2006. Petrogenesis of mantle peridotites from the Izu-Bonin-Mariana (IBM) forearc. *Ofioliti*, 31, 2, 189-206. DOI: https://doi.org/10.4454/ofioliti.v31i2.340

Zimmer, M., Kröner, A., Jochum, K.P., Reischmann, T., Todt, W. 1995. The Gabal Gerf complex: a Precambrian N-MORB ophiolite in the Nubian Shield, NE Africa. *Chemical Geology*, 123, 29–51. DOI: https://doi.org/10.1016/0009-2541(95)00018-H